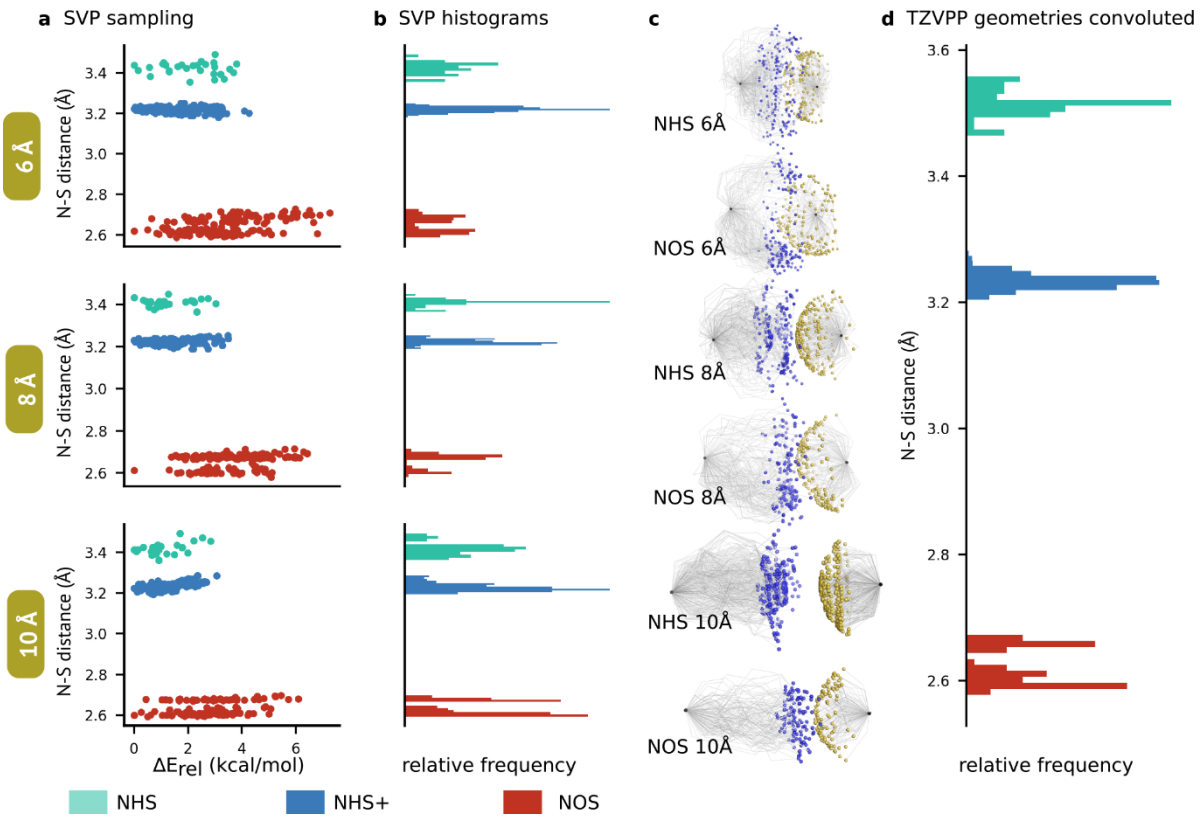

ED Figure 1. Computed structural information for conformers of Lys and Cys residues with and without the NOS bond, using different alpha-carbon distances (6 Å, 8 Å and 10 Å). The residues are computed as models, truncated at the alpha-carbons. The sampled structures at the semi-empirical level were refined at the B3LYP-D3(BJ)/def2-SVP level of theory (more details in SI), with the lowest conformers being reoptimised with a larger basis (def2-TZVPP). We have considered three different conformers: NOS - covalent bonding between the residues, NHS - hydrogen bond with the Lys deprotonated and NHS+ - hydrogen bond with the Lys protonated. (**a**) N-S distance (in Å) as a function of the relative conformer stability within each group computed with the SVP basis; (**b**) histogram for the SVP basis results; (**c**) overlap of SVP optimised structures for NHS and NOS; (**d**) histogram for all structures with the TZVPP basis.

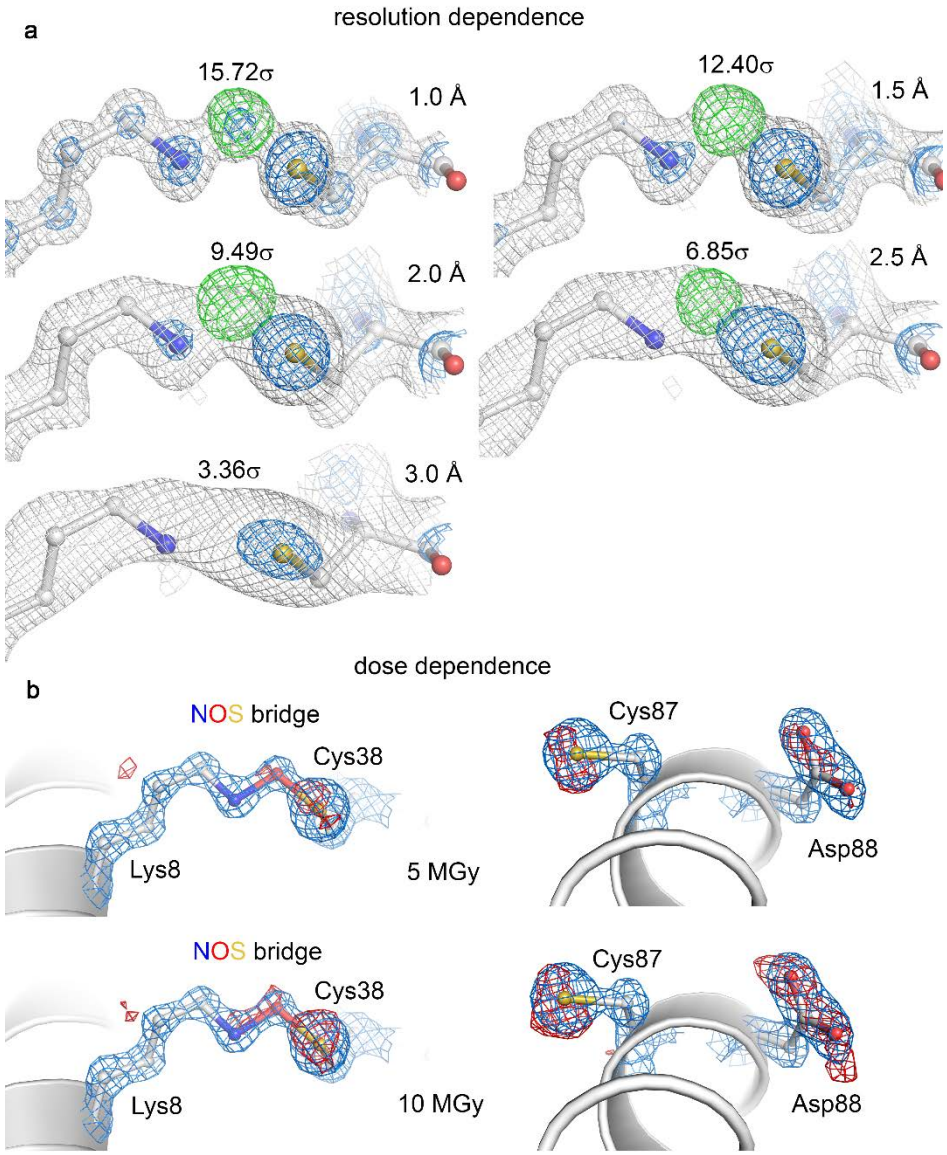

ED Figure 2. Detectability of NOS bridges in protein crystal structures in dependence from resolution and deposited dose. (**a**) Resolution dependence. A previously determined sub-ångstrøm resolution crystallographic dataset obtained for *Neisseria gonorrheae* transaldolase (pdb code 6XZ4) [9], which forms an allosteric NOS bridge between Lys8 and Cys38, was truncated at different resolutions from 1.0-3.0 Å as indicated. For refinement, the lysine and cysteine residues were modeled without the bridging oxygen atom. The calculated structural models and 2mFo-DFc electron density (blue: 3σ, grey: 1σ) and mFo-DFc difference electron density (green: 5σ) maps are shown. The respective intensities of the positive peaks in the difference electron density maps are indicated. Note the loss of structural information regarding the bridging oxygen atom with decreasing resolution. (**b**) Dose dependence. Crystallographic datasets for a single crystal of *Neisseria gonorrheae* transaldolase were collected at different doses between 0.5 and 10 MGy at cryogenic temperature. The refined structural models of the NOS bridge formed between Lys8 and Cys38 and of a neighboring helix bearing residues Cys87 and Asp88 are shown for datasets obtained at doses of 5 MGy and 10 MGy. The respective 2mFo-DFc electron density maps are contoured at 2σ. The calculated difference in intensity in the electron density maps relative to that obtained for a dose of 0.5 MGy is shown in red at a contour level of 3σ. Note the progressive loss in intensity for Cys87 and Asp88 with increasing dose, which indicates “radiation damage”. For the NOS bridge, radiation damage sets in at high doses of 10 MGy.

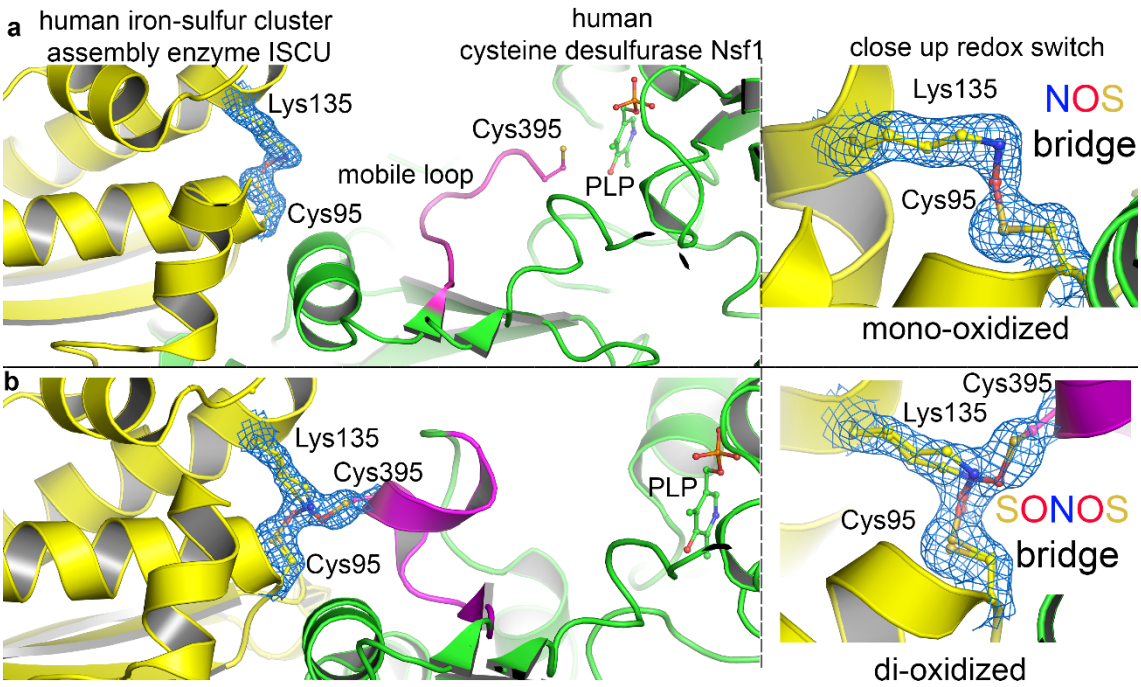

ED Figure 3. NOS and SONOS bridges in the human Fe/S cluster biosynthesis complex. (**a**) Structure of the complex consisting of iron-sulfur cluster assembly enzyme ISCU (highlighted in yellow) and cysteine desulfurase Nsf1 (highlighted in green) in the mono-oxidized state with an intramolecular NOS bridge between Cys95 and Lys131 of ISCU (pdb code 6UXE). A mobile loop from Nsf1 with catalytic residue Cys395 catalyzing sulfide transfer from the PLP cofactor at the active site of Nsf1 to ISCU is indicated in magenta. Left panel: structural overview. Right panel: close-up of the redox switch site. For residues Cys95 and Lys135, the structural models are superposed with the corresponding 2mFo-DFc electron density maps at a contour level of 1σ. Note that Cys395 visits the active site of Nsf1. (**b**) Structure of the complex in the di-oxidized state with a SONOS bridge formed between Cys95 and Lys131 of ISCU and Cys395 of Nsf1 (pdb code 6WI2, also observed in 6WIH). Left panel: structural overview. Right panel: close-up of the redox switch site. For residues Cys95, Lys135 and Cys395 the structural models are superposed with the corresponding 2mFo-DFc electron density maps at a contour level of 1σ. Competitive refinements (SONOS bridge only, 2 separate NOS bridges, mixture of SONOS and NOS) indicate a mixture of the SONOS bridge (refined occupancy 60%) and the NOS bridge between Lys135 and Cys95 (refined occupancy 40%) for this dataset.

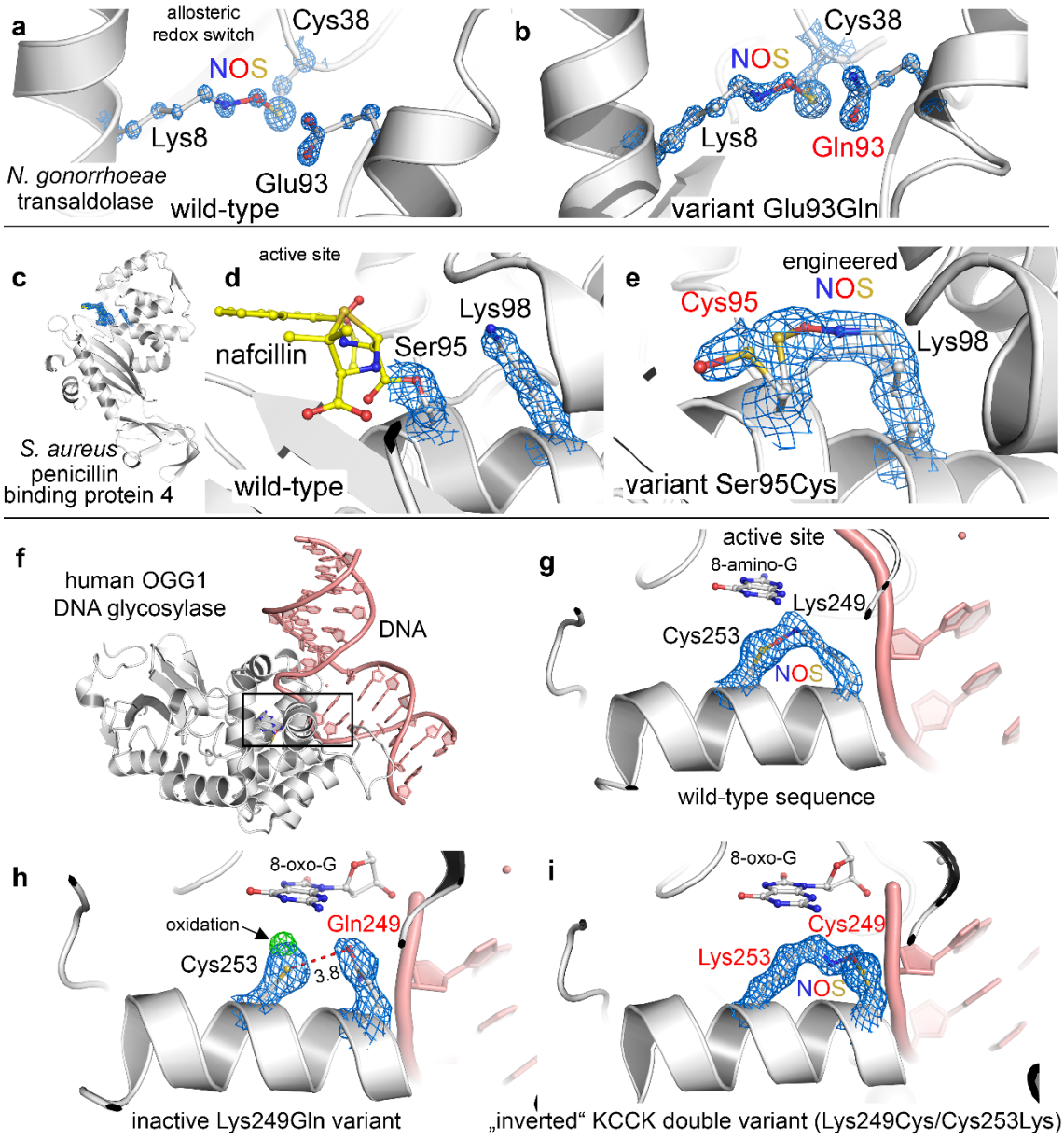

ED Figure 4. Structural requirements for formation and engineering of NOS bridges. (**a**, **b**) Structure of the allosteric NOS bridge in *Neisseria gonorrhoeae* transaldolase wild-type (a, pdb code 6XZ4) [9] and variant Glu93Gln (b, this study) showing NOS residues Lys8 and Cys38 as well as neighboring residue 93. The structural models of Lys8, Cys38 and Glu93 or Gln93 are superposed with the corresponding 2mFo-DFc electron density maps at 3σ. Note that NOS bridge formation does not require the presence of a catalytic residue at position 93. (**c**, **d**, **e**) An unintentionally engineered NOS bridge in *Staphylococcus aureus* penicillin binding protein 4 showing the overall protein structure (c) and a close-up of the active site with catalytic residues Ser95 (nucleophile) in linkage with nafcillin and Lys98 (d, pdb code 5TY2). In variant Ser95Cys (e), where the catalytic Ser95 has been replaced by cysteine, an NOS bridge was formed between introduced Cys95 and Lys98. The structural models of residues 95 and 98 are superposed with the corresponding 2mFo-DFc electron density maps at 1σ. In variant Ser95Cys, residue 95 was modeled in two alternative conformations. (**f**-**i**) NOS bridges in the human DNA glycosylase OGG1. (**f**) Overall structure of OGG1 in complex with DNA (pdb code 1M3Q). (**g**) Close-up of the active site showing catalytic residue Lys249 (Schiff-base with DNA) and neighboring residue Cys253 forming an NOS bridge. The structural models of Lys249 and Cys253 are superposed with the corresponding 2mFo-DFc electron density maps at 1.5σ. (**h**)

Active site structure of inactive OGG1 variant Lys249Gln (pdb code 1EBM), in which the catalytic lysine had been replaced by glutamine. The structural models of Gln249 and Cys253 are superposed with the corresponding 2mFo-DFc electron density maps in blue at 1.5σ and the mFo-DFc difference electron density map in green at 3σ. Note that Gln249 and Cys253 form a H-bond rather than an NOS bridge and that Cys253 is likely to be oxidized as indicated by the positve peak in the difference electron density map. (**i**) Active site structure of OGG1 KCCK double variant Lys249Cys/Cys253Lys (pdb code 2XHI), in which the sequence positions of the NOS-bridge-forming Lys and Cys residues are inverted. The structural models of Cys249 and Lys253 are superposed with the corresponding 2mFo-DFc electron density maps at 1.5σ. Note the presence of the NOS bridge in this “inverted” variant akin to the wild-type sequence argueing against a mechanism, where catalysis is provided by neighboring residues for the NOS bridge to form.

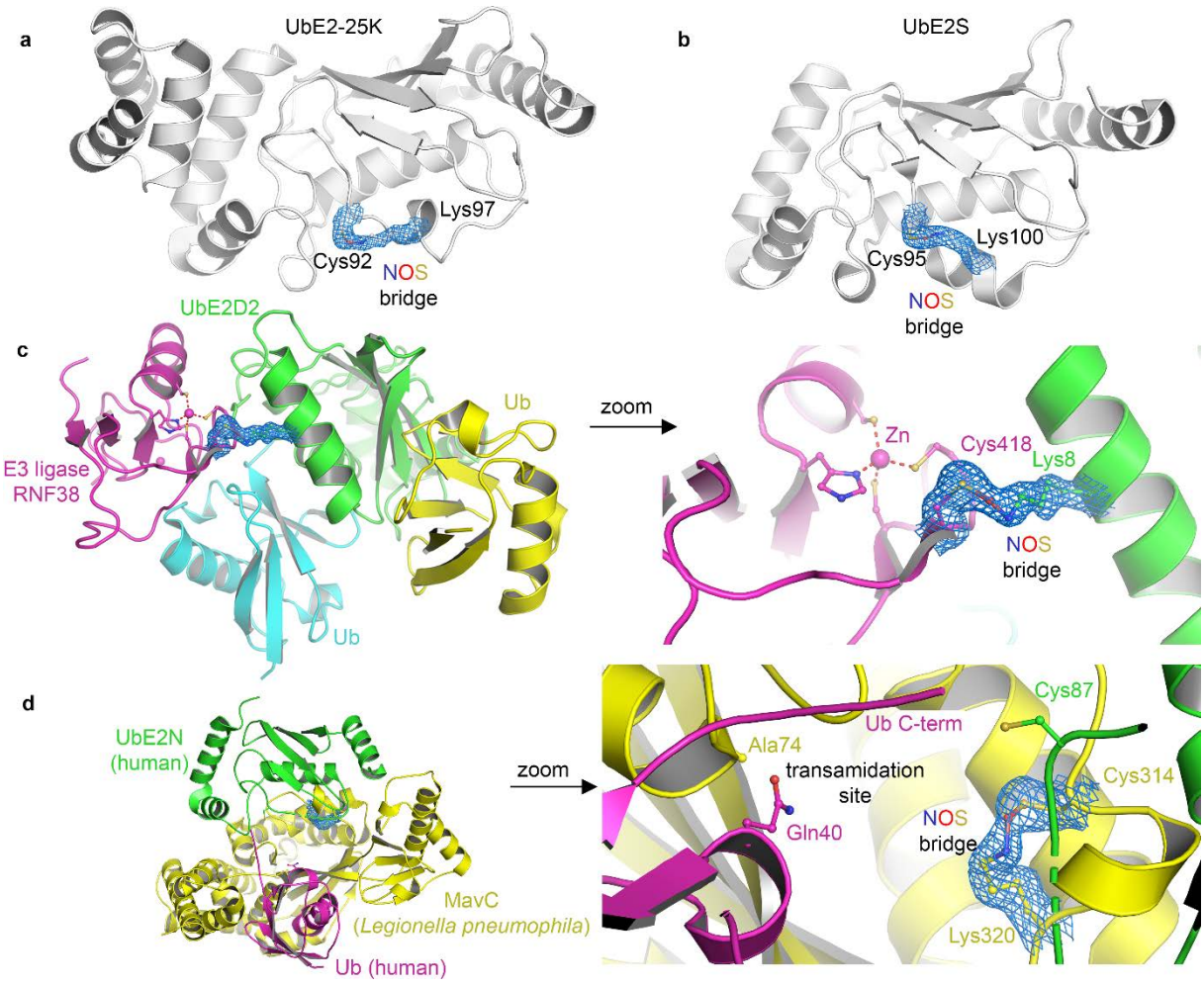

ED Figure 5. NOS bridges in proteins from the ubiquitin system. (**a**) Human ubiquitin-conjugating enzyme E2-25K (UbE2-25K) with an NOS bridge formed between catalytic residue Cys92 and Lys97, a potential auto-ubiquitination site (pdb code 3E46). The structural models of the NOS bridge-forming lysine and cysteine residues are superposed with the corresponding 2mFo-DFc electron density maps at 1σ. (**b**) Human ubiquitin-conjugating enzyme E2-S (UbE2S) with an NOS bridge formed between catalytic residue Cys95 and Lys100, a potential auto-ubiquitination site (pdb code 6QHK). The structural models of the NOS bridge-forming lysine and cysteine residues are superposed with the corresponding 2mFo-DFc electron density maps at 1σ. (**c**) Complex between ubiquitin-conjugating enzyme E2 D2 (UbE2D2), E3 ring ligase RNF38 and two ubiquitin (Ub) molecules (pdb code 4V3L). Left: Overall structure of the complex showing the proteins in individual colors. Right: Close-up of the intermolecular NOS bridge formed between Lys8 of E2 and Cys418 of E3. Note the proximity of the NOS bridge with respect to the Zn^{2+}-binding site of E3. The structural models of the NOS bridge-forming lysine and cysteine residues are superposed with the corresponding 2mFo-DFc electron density maps at 1σ. (**d**) Structure of a complex between MavC from *Legionella pneumophila* in complex with human ubiquitin-conjugating enzyme E2 N (UbE2N) and human ubiquitin (Ub) (pdb code 6ULH). MavC is a bacterial effector that inactivates the human ubiquitin system by catalyzing a transamidation reaction between Lys92 of UbE2N and Gln40 of Ub forming a dead-end complex [36]. Left: Overall structure of the complex showing the proteins in individual colors. Right: Close-up of the intramolecular NOS bridge in MavC formed between Lys320 and Cys314. Note the proximity of the NOS bridge with respect to the transamidation site. The structural models of the NOS bridge-forming lysine and cysteine residues are superposed with the corresponding 2mFo-DFc electron density maps at 1σ.

Organism/species	Protein	Function	Redox switch	Mechanism	Disease/comments
Human Pathogens					
Viruses					
SARS-CoV-2	Main protease (Mpro)	Polyprotein processing	NOS (K61-C22) **pdb 6XMK** SONOS (C44-K61-C22) **pdb 7JR4**	allosteric mobile Cys (C44)	COVID-19
SARS-CoV	Main protease (Mpro)	Polyprotein processing	NOS (K61-C22) **pdb 3SND**	allosteric	SARS
Human adenovirus	Fiber protein	Binding to host receptor	NOS (K295-C333) **pdb 1UXB**	allosteric	Adenoviral keratoconjunctivitis
Human cytomegalovirus	Nuclear egress complex pUL50	Virus maturation and assembly	NOS (K132-C54) **pdb 6T3X**	allosteric	HCMV infection (herpes)
Bacteria					
Neisseria gonorrhoeae	transaldolase	Sugar metabolism	NOS (K8-C38) **pdb 6ZX4**	allosteric	Gonorrhoea
Neisseria meningitidis	transaldolase	Sugar metabolism	NOS (K8-C38) Sequence homology	allosteric	Bacterial meningitis and septicemia
Vibrio cholerae	Oxaloacetate decarboxylase	Na^+ pump/ATP biosynthesis	NOS (K178-C148) **pdb 2NX9**	Catalytic Lys (CO_2 transfer)	Cholera
Staphylococcus aureus	Pyruvate carboxylase	Gluconeogenesis	NOS (K741-C705) Structural homology **pdb 3HO8**	Catalytic Lys (CO_2 transfer)	Bacterial superinfection
Listeria monocytogenes	Pyruvate carboxylase	Gluconeogenesis	NOS (K710-C674) Structural homology **pdb 4QSK**	Catalytic Lys (CO_2 transfer)	Listeriosis
Listeria monocytogenes	Transcriptional regulator PrfA	Regulation gene expression	NOS (K163-C205) **pdb 6EUT**	allosteric	Listeriosis
Mycobacterium tuberculosis	DAHP synthase (DAHPS)	Amino acid metabolism	NOS (K133-C440) **pdb 3RZI**	substrate binding	Tuberculosis
Pseudomonas aeruginosa	DAHP synthase (DAHPS)	Amino acid metabolism	NOS (K115-C423) Structural homology **pdb 5UXN**	substrate binding	Pneumonia
Ruminococcus gnavus	Metal binding protein	unknown	NOS (K128-C100) **pdb 3U7Z**	allosteric	Crohn's disease
Pseudomonas aeruginosa	Dihydrodipicolinate synthase (putative)	Lysine biosynthesis	NOS (K185-C227) **pdb 3NA8**	catalytic Lys (Schiff base)	Pneumonia
Acinetobacter sp. DL-28	L-ribose isomerase	Sugar metabolism	NOS (K93-C91) **pdb 4Q0P**	substrate binding (Lys)	Nosocomial infections, pneumonia
Salmonella typhimurium	Multidrug resistance regulator RamR	Regulation gene expression	NOS (K63-C67) **pdb 6IE9**	allosteric	Gastroenteritis, typhoid fever
Legionella pneumophila	Effector MavC	Inactivation of human Ub system	NOS (K320-C314) **pdb 6ULH**	Proximal to trans-glutaminase site	Legionnaires' disease
Streptomyces sp. K15	DD-transpeptidase (penicillin binding protein)	Cell wall biosynthesis	NOS (K38-C98) **pdb 1SKF**	catalytic Lys (acid-base)	target protein of β-lactam antibiotics
Parasites					
Trypanosoma cruzi	Farnesyl diphosphate synthase	Isoprenoid biosynthesis	NOS (K158-C154) **pdb 6SDP**	allosteric	Chagas disease
Trypanosoma brucei	Ornithine decarboxylase	Polyamine biosynthesis	NOS (K69-C360) Structural homology **pdb 1F3T**	Catalytic Lys Schiff-base PLP	African sleeping sickness
Plant pathogens					
Viruses					
Paramecium bursaria Chlorella Virus	Arginine decarboxylase	Polyamine biosynthesis	NOS (K48-C324) **pdb 2NV9**	Catalytic Lys Schiff-base PLP	Infection of algae, cell lysis and death
Bacteria					
Xanthomonas campestris	Sucrose hydrolase	Sugar metabolism	NOS (K321-C174) **pdb 2WPG**	Proximal to active site	"Black rot" in cruciferous vegetables
Xanthomonas axonopodis	Sucrose hydrolase	Sugar metabolism	NOS (K320-C173) **pdb 3CZG**	Proximal to active site	Bacterial pustule of soybean

ED Table 1. NOS/SONOS bridges in proteins from human and plant pathogens. Information is provided for the protein identity, the origin of the protein, the biological function of the protein, the detected switch type (NOS or SONOS) with residues involved and relevant pdb codes, the suggested mechanism of the redox switch and relevant diseases associated with the identified species. Proteins identified based on structural homology are highlighted in gray shading. The complete list of all proteins with detected NOS bridges is provided in SI Data 1.

Organism	Protein	Function	Redox switch	Mechanism	Disease/comments
DNA repair					
Homo sapiens	OGG1	DNA repair (excision 8-oxo-dG)	NOS (K249-C253) **pdb 1M3Q**	Catalytic Lys (Schiff-base)	Various cancers
Homo sapiens	Metalloprotease Spartan	DNA repair (cleavage of DNA-protein crosslinks)	NOS (K184-C75) **pdb 6MDW**	Proximal to active site	Ruijs–Aalfs syndrome (premature aging and cancer)
Protein biosynthesis and degradation					
Homo sapiens	Density regulated protein	Regulation of translation on ribosome	NOS (K125-C154) **pdb 6VPQ**	Lys on functional loop ('basic loop')	Asperger syndrome Cancer (conjunction with MCTS1)
Homo sapiens	Lysine methyltransferase METTL21C	Methylation of alanine tRNA synthetase	NOS (K76-C160) **pdb 4MTL**	allosteric	Chromosome 4q21 Deletion Syndrome Inclusion body myositis Osteoporosis
Homo sapiens	Ubiquitin-conjugating enzyme E2-25kDa	ubiquitin-dependent protein degradation	NOS (K97-C92) **pdb 3E46**	Catalytic Cys (Catalytic Lys)	Alzheimer's disease Huntington disease
Homo sapiens	Ubiquitin-conjugating enzyme E2 S	ubiquitin-dependent protein degradation (mitosis, meiosis)	NOS (K100-C95) **pdb 6QHK**	Catalytic Cys (Catalytic Lys)	Various cancers
Homo sapiens	Ubiquitin-conjugating enzyme E2 D2 E3 ligase RNF38	ubiquitin-dependent protein degradation	NOS ($K8^{E2}$-$C418^{E3}$) Interchain **pdb 4V3L**	Proximal to Zn^{2+} cluster of E3	Various cancers
Transcription regulation					
Mus musculus (conserved in human)	Tubby protein	Transcription regulation, signaling	NOS (K339-C370) **pdb 1I7E**	allosteric	Maturity-onset obesity Retinal dystrophy
Mus musculus (conserved in human)	Homeobox protein Hox-A9	Transcription regulation (cell fate & embryonic patterning)	NOS (K207-C210) **pdb 1PUF**	DNA Binding (Lys)	Acute myeloid leukemia
Homo sapiens	PHD finger protein 2	Transcription regulation Histone demethylation	NOS (K266-C240) **pdb 3PU8**	Substrate binding (Lys) (α-ketoglutarate)	Culler-Jones syndrome, cancer Autism Spectrum Disorder
Homo sapiens	Histone-lysine N-methyltransferase SUV420H2	Transcription regulation Histone methylation	NOS (K122-C111) **pdb 3RQ4**	Proximal to substrate binding site (SAM)	Various cancers
Mus musculus (conserved in humans)	Interferon gamma-inducible protein 16	dsDNA sensing, innate immune response	NOS (K267-C390) **pdb 5YZP**	allosteric	Autoimmune disorders as e.g. primary Sjögren's syndrome (pSS), Cancer
Signaling					
Rattus norvegicus (conserved in humans)	Galectin-1	Signaling, regulation of cell growth and differentiation, immune response	SONOS (C17-K100-C89) **pdb 4GA9**	allosteric	Various cancers, inflammation, allergies
Homo sapiens	Hematopoietic cell receptor CD69	Lymphoid activation, signaling	NOS (K146-C173) **pdb 1E8I**	unknown	Inflammatory diseases (e.g. inflammatory bowel disease)
Homo sapiens	Tyrosine-protein kinase JAK2, pseudokinase domain	Signaling, tyrosine phosphorylation	NOS (K650-C747) **pdb 4FVQ**	allosteric	Bone marrow diseases (Myeloproliferative neoplasms, leukemia)
Gallus gallus (conserved in humans)	Focal adhesion kinase 1	Signaling, regulation cell migration and motility	NOS (K255-C257) **pdb 6CBO**	allosteric	Various cancers
Homo sapiens	Casein kinase I isoform delta	Ser/Thr kinase Signaling in cell division, apoptosis, inflammation	NOS (K57-C71) **pdb 6F1W**	Proximal to ATP binding site	Various cancers Alzheimer's disease Parkinson's disease
Homo sapiens	Dual specificity protein kinase CLK1	Regulation RNA splicing	NOS (K174-C151) **pdb 6FT9**	allosteric	Various cancers Alzheimer's disease
Homo sapiens	Casein kinase gamma 3	Signaling (Ser/Thr kinase)	NOS (K48-C51) **pdb 2IZU**	allosteric	Various cancers Fibrosis
Homo sapiens	TBC1 domain family member 7	Signaling (GTPase activation), regulation cell growth & differentiation	NOS (K233-C286) **pdb 3QWL**	Ligand binding (metal ion)	Macrocephaly/mega-lencephaly syndrome Tuberous sclerosis
Homo sapiens	Leucine carboxylmethyl-transferase-1	Signaling, Regulation PP2A activity	NOS (K62-C36) **pdb 3IEI**	Proximal to substrate SAM	Alzheimer's disease
Rattus norvegicus (conserved in humans)	Rabphilin-3A	Regulation of exo- and endocytosis (neurotransmission)	NOS (K423-C473) **pdb 4NP9**	Effector IP3 binding (Lys) proximal to Ca^{2+} binding site	Levodopa-induced dyskinesias, Martsolf Syndrome (MARTS)
Doryteuthis pealeii	Calexcitin	Signaling in learning and memory, regulation K^+ channels	NOS (K41-C24) **pdb 2CCM**	proximal to Ca^{2+} binding site	Alzheimer's disease
Homo sapiens	diphosphoinositol phosphohydrolase 1	Regulation of inositol diphosphate signaling	NOS (K74-C68) **pdb 6PCK**	allosteric	Renal dysplasia, cerebellar hypoblasia
Biosynthesis sulphur-containing cofactors and rare amino acids					
Homo sapiens	iron-sulfur cluster assembly enzyme ISCU2	Iron-sulfur cluster biogenesis	NOS (K135-C95) **pdb 6UXE**	Catalytic Cys (C95)	Mitochondrial myopathy Friedreich's ataxia (FRDA) Sideroblastic anemia
Homo sapiens	Cysteine desulfurase NFS1 iron-sulfur cluster assembly enzyme ISCU2	Iron-sulfur cluster biogenesis	SONOS (C381-K135-C95) Interchain **pdb 6WI2**	Catalytic Cys (C381, C95) Mobile Cys (C381)	Mitochondrial myopathy Friedreich's ataxia (FRDA) Sideroblastic anemia
Homo sapiens	S-adenosylmethionine synthase isoform type-2	S-Adenosylmethionine biosynthesis	NOS (K307-C149) **pdb 6FBP**	allosteric	Familial Thoracic Aortic Aneurysm and Aortic Dissection (FAA) Various cancers
Homo sapiens	Selenophosphate synthetase 1	Redox homeostasis, selenium salvage pathway	NOS (K27-C31) **pdb 3FD5**	On catalytic loop	Ivic Syndrome Ischiocoxopodopatellar Syndrome
Homo sapiens	Selenophosphate synthetase 2	Selenocysteine/selenoprotein biosynthesis	NOS (K58-C62) sequence homology	On catalytic loop	Keshan Disease Ischiocoxopodopatellar Syndrome
Cytoskeleton					
Gallus gallus (conserved in human)	Actin capping protein alpha 1	Regulation of actin filament dynamics	NOS (K135-C147) **pdb 3AA1**	allosteric	Degenerative diseases cancer
Mus musculus (conserved in human)	Profilin-2	Microfilament nucleation and polymerisation	NOS (K126-C16) **pdb 2V8F**	Proximal to ligand binding site	Neurological and behavioural diseases

ED Table 2. Human proteins (or from animal models) with NOS bridges classified according to their cellular function. Information is provided for the protein identity, the origin of the protein, the biological function of the protein, the detected switch type (NOS or SONOS) with residues involved and relevant pdb codes, the suggested mechanism of the redox switch and relevant diseases associated with the identified species. Proteins identified based on sequence homology are highlighted in gray shading. In case the identified protein originates from an animal model system, a putative sequence conservation of the NOS residues in the human orthologue is indicated. The complete list of all proteins with detected NOS bridges is provided in SI Data 1.